Arthritis Research & Therapy

RESEARCH

Open Access

Effects of chronic ankle instability after grade I ankle sprain on the post-traumatic osteoarthritis

Yan Du[1,2], Shuo Wang[1,3], Fanlei Yang[1], Hao Xu[1], Yu Cheng[1*] and Jia Yu[1,2*]

Abstract

Background Untreated acute ankle sprains often result in chronic ankle instability (CAI) and can ultimately lead to the development of post-traumatic osteoarthritis (PTOA). At present, a typical animal model of ankle instability in mice is established by transecting the ligaments around the ankle joint. This study aimed to establish a grade I acute ankle sprain animal model by rapid stretching of peri-ankle joint ligaments. Furthermore, we tried to explore the pathophysiological mechanism of ankle osteoarthritis.

Methods In all, 18 male C57BL/6 J mice (7 weeks) were randomly divided into three groups: calcaneofibular ligament (CFL) laxity group, deltoid ligament (DL) laxity group, and SHAM group. One week after the surgical procedure, all mice were trained to run in the mouse rotation fatigue machine daily. The mice were tested on the balance beam before surgery and three days, 4 weeks, 8 weeks, and 12 weeks after surgery. Footprint analyses were performed on each mouse before surgery and 12 weeks after surgery. Micro-CT scanning was then performed to evaluate the degeneration of ankle joints and histological staining was performed to analyze and evaluate PTOA caused by ankle joint instability.

Results After surgery, the mice in the CFL and DL laxity groups took longer to cross the balance beam and slipped more often than those in the SHAM group ($p < 0.05$). The step length and width in the CFL and DL laxity groups were significantly shorter and smaller than those in the SHAM group 12 weeks after surgery ($p < 0.05$). There was a significant increase in the bone volume fraction (BV/TV) in the CFL and DL laxity groups compared with the SHAM group ($p < 0.05$). Histological staining results suggested obvious signs of PTOA in the CFL and DL laxity groups.

Conclusions Based on CFL and DL laxity in a mouse ankle instability model, this study suggests that grade I ankle sprain can contribute to chronic ankle instability, impair motor coordination and balance, and eventually lead to PTOA of ankle with significant degeneration of its adjacent joints.

Keywords Ligament laxity, Ankle sprain, Ankle instability, Post-traumatic osteoarthritis, Biomechanics

*Correspondence:
Yu Cheng
chengyusz@126.com
Jia Yu
jiayu@suda.edu.cn
Full list of author information is available at the end of the article

Background

Ankle sprain (AS) is one of the most common sports injuries in daily activities. After injury, clinical symptoms such as ecchymosis, hematoma, and tenderness on the lateral side of the hind foot often occur. It is estimated that 10,000 individuals are injured every day in the United States [1], and sports-related injuries account for 15% to 45% of all injuries [2]. The medical costs for treating ankle sprains in the United States reach $4.2 billion annually [3–5]. Furthermore, failure to detect ankle injuries can promptly cause chronic ankle instability (CAI), a common condition after ankle sprains, occurring in approximately 74% of ankle sprains [6]. The ultimate outcome of long-term CAI is pain, dysfunction, joint deformities, and post-traumatic osteoarthritis (PTOA) [7–9], which can even affect adjacent joints in severe cases [10]. This not only seriously affects the personal quality of life of patients but also aggravates the economic burden on families and affects the economic development of the society and the country. Therefore, early diagnosis and treatment of ankle instability to prevent its further escalation to irreversible PTOA is an urgent issue that needs to be addressed.

The ankle joint is a complex joint that is the core structure of the foot and plays a pivotal role in maintaining the body's stability during daily activities [11]. Furthermore, the integrity of the ankle joint structure and its surrounding ligaments are the basis for its normal function. The lateral ligament of the ankle joint mainly comprises the anterior talofibular ligament (ATFL), calcaneofibular ligament (CFL), and posterior talofibular ligament (PTFL) [12]. In epidemiological investigations, we have found that approximately 35% of all lateral ankle ligament injuries caused by ankle sprains result in the CFL damage [13]. The medial ligament of the ankle joint is the deltoid ligament (DL), which consists of superficial and deep portions and extends from the inner ankle to the talus, calcaneus, and navicular bones [14, 15]. Under physiological load, the DL is considered to be the primary static stabilizer of the ankle joint and can prevent external rotation and lateral displacement of the talus. Studies have shown that complete rupture of the superficial and deep portions of the DL can cause instability of the ankle joint and abnormal movement of the talus [16–18].

To explore the mechanism of ankle joint cartilage degeneration, researchers have conducted extensive research including cadaver specimen experiments, finite element model analysis, and other experiments. However, given the ethical limitations and experimental conditions, it is often difficult to conduct long-term in vivo experiments on volunteers. Moreover, it is often difficult to determine a quantitative correlation between the cartilage tissue stress and biological immunohistochemistry during pathological degeneration without changing their physiological state. Preclinical animal models can better meet this demanding requirement, and various detection methods have been used to assess the degree of osteoarticular cartilage damage and degeneration at macro, micro, and nano levels [19].

Among many commonly used experimental animals, horses, cows, and sheep have a hoof-walking gait, and cats and dogs have a toe-walking gait. In contrast, mice and humans both have a plantar-walking gait. Mice also have a highly similar hind limb skeletal system and cartilage structure to human lower limbs [20]. In the comparison of dynamics, the neuromuscular movement of mice also has a relatively similar regulation mode to that of humans [21]. Furthermore, the anatomical structure of ankle joint and the distribution of ligaments around the ankle joint are identical between both mice and humans [22]. An increasing number of scholars have recently attempted to use mice to establish the biomechanical animal model of ankle sprain instability. Chang et al. successfully established three types of ankle osteoarthritis models with ligament transection by cutting the ligaments around the ankle joint in mice [20]. In the early stage, our research group [10] used the instability of the subtalar joint complex in mice to successfully establish a PTOA model by cutting ligaments such as the cervical ligament (CL), ATFL, and DL. However, in actual life, it is more common to encounter grade I sprains of the ankle joint, namely mild sprains, with visible ligament stretching and relaxation but not visible tears. Only grade II/III sprains of the ankle joint, i.e., moderate to severe sprains, cause locally visible ligament tears or ruptures [23]. Accordingly, whether the instability of the ankle joint caused by mild sprains affects the foot and ankle biomechanics, causing instability of the ankle joint and cartilage damage, is unclear.

Ankle sprains often occur acutely (within 40 ms) [24], and ligaments are typical biological tissues, with the most essential characteristic of viscoelasticity. This indicates that the stress response during an ankle sprain is time-dependent [25]. In this study, we aimed to use the rapid ligament stretching method to simulate ankle sprains, resulting in ligament relaxation type damage, and investigated whether grade I sprains also lead to CAI. We evaluated the macroscopic behavioral stability of mice through the balance beam experiments and gait footprint analysis. Furthermore, tissue specimens were evaluated for ankle joint inflammation via micro-CT, Hematoxylin and Eosin (H&E) staining, Safranin O-Fast Green (SOFG) staining, Toluidine blue (TB) staining, and immunohistochemical (IHC) staining.

Methods

Animals

In all, 18 male C57BL/6 J [age, 7 weeks; weight ranging from 18.5 to 22.3 g (mean body weight: 21.8 g)] were acquired from JOINN Laboratory [SCXK (Su) 2018–0006, Suzhou, China] and were randomly assigned to six cages, with an average of three mice per cage. The mice were housed in a specific pathogen-free (SPF) environment, with a light/dark cycle of 12 h/12 h and constant temperature and humidity of 18–22 °C and 40%–70%. The mice moved freely in cages and received sufficient food and water. The padding in the cage was regularly checked and the health status of the mice was observed every day. In the first week, the mice were allowed to adapt to the new feeding environment and were trained to crawl through the balance beam and U-shaped pipes. Before initiating the official surgery, we randomly divided 18 mice into three groups: the CFL laxity group ($n=6$), the DL laxity group ($n=6$), and the SHAM group ($n=6$). The Animal Experiment Ethics Committee of Soochow University approved the use and handling of animals in this study.

Surgical procedures

At the age of 8 weeks, all mice were weighed and placed in a closed container containing isoflurane for anesthesia by inhaling. When the mice were under deep anesthesia (corneal reflex and pain reflex were observed to determine the degree of anesthesia), a shaving machine was used to remove the hair on the right hind limb of the mice. The right hind limbs of the mice were disinfected with strict accordance with the principles of surgical disinfection. After disinfection, the mice were placed on the microsurgical table, and the anatomical structure of the right hind foot of the mice was observed under the microscope (Fig. 1A).

In the CFL laxity group, a 7-mm longitudinal incision was made on the skin outside the right ankle to separate the subcutaneous tissue, exposing the ankle and subtalar joints. The CFL connecting the fibula and calcaneus could be seen. Subsequently, the ligament was attached to a polishing hook. After preliminary study for mimicking grade I acute ankle sprain by rapid stretching of DL or CFL, appropriate weight and height were chosen to cause visible ligament stretching and approximately 20% relaxation but no visible tears on microscope evaluation. A weight of 15 g rapidly pulled the ligament down by 20 cm (0.0297 kg·m/s impulse) to cause relaxation traction on the CFL. In the DL laxity group, a longitudinal incision of approximately 8 mm in length was made vertically downward at the posterior medial skin of the right ankle in mice to isolate subcutaneous tissue and locate DL from the anterior medial malleolus to the scaphoid bone and talus. The middle of the ligament was then attached to a polishing hook. A weight of 5 g rapid pulled the ligament down by 15 cm (0.00855 kg·m/s impulse) to cause relaxation traction on the DL. In the SHAM group, the skin and fascia were dissected, but no ligament relaxation was performed (Fig. 1B).

After the operation, the incision was rinsed with sterile saline, and the fascia and skin were sequentially sutured. Finally, the incision was sterilized with a cotton ball containing Aner iodine. After waking up in the cage, the mice can move freely and consume food and water. The

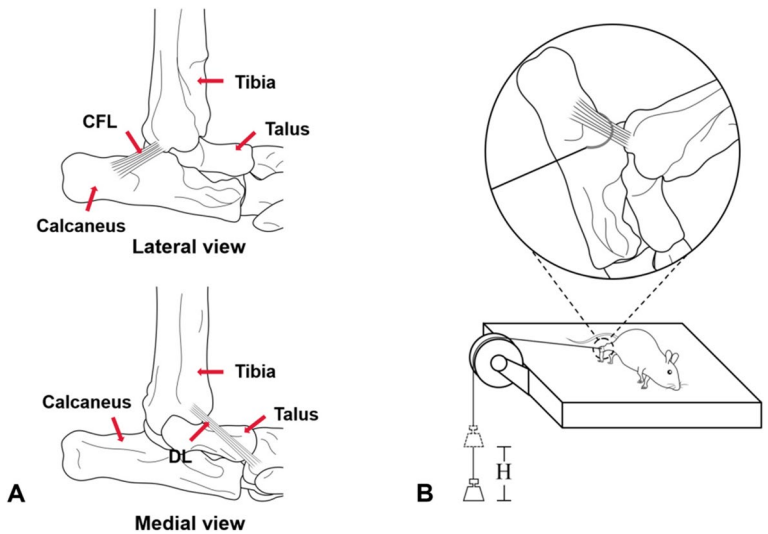

Fig. 1 Establishment of animal models. **A** Schematic diagram of the calcaneofibular ligament (CFL) and the deltoid ligament (DL). **B** Schematic diagram of establishing the grade I ankle sprain mouse model by rapid stretching ankle ligament with a weight

incisions were disinfected twice a day for one week after surgery with cotton balls containing Aner iodine, and the postoperative conditions of mice were closely monitored. One week after operation, the mice were trained to run five times a week (30 min/day, 7.5 m/min) for 12 weeks using a Rotation fatigue machine.

Balance assessments

The motor coordination and balance in mice were assessed by measuring the ability of the mice to reach a safe platform through a beam tilted 15°. A round wooden beam of 1 m in length and 20 mm in diameter was used, with one end of the beam connected to a camera clip and the other end connected to the closed box. Before surgery, the mice were trained for a week so that they could run skillfully from one end of the wooden beam to the other, ensuring that the mice could pass the wooden beam without interruption when the experiment was officially conducted. Before the experiment, the mice were placed at the starting point of the photographic bracket. While the mouse starts crawling, the timer was pressed to record the time it takes (in seconds) for the mice to crawl from the starting point to the endpoint without stopping and the camera recorded the number of times the right hind foot of each mouse slid (times). The mice were allowed to pass through the wooden beam for up to 60 s; the time the mice took to cross the wooden beam and the number of times the right back foot slipped off the wooden beam were the dependent variables [26, 27]. The balance beam experiment was conducted before the operation and three days, one week, 4 weeks, 8 weeks, and 12 weeks after the operation. Each mouse was required to complete three tests during each experiment, and the subsequent analysis was based on the average value of the three tests.

Footprint analysis

Before surgery and 12 weeks after surgery, the front and hind feet of all mice were coated with different pigments. The mice were placed on a U-shaped track with a length of 50 cm, a width of 10 cm, and a height of 10 cm, from which their footprints were obtained. In the analysis of footprints, the footprints of the first and last step left by mice on the gait paper were first excluded, and the three consecutive and clear steps in the middle were intercepted for the measurement and statistics of step length and width.

Micro-CT scanning

The mice were euthanized 12 weeks after surgery, and the right hind ankle joint was resected. The skin and some soft tissues of the ankle joint were removed with surgical forceps and fixed in a centrifuge tube containing 10% neutral formalin solution for 48 h. After fixation, the samples were placed in batches (4 samples at each time) in a specially designed sponge tank. They were scanned using a high-resolution microcomputer tomography (SkyScan 1176, Aartselaar, Belgium) machine with the following scanning parameters:50 kV, 200 Ma, and 9 μm resolution. After scanning, the scanning images are processed and reconstructed using NRecon and DataView software. In CTAN software, the cartilage layer to subchondral bone layer of ankle joint and subtalar joint were selected as region of interest (ROI) for quantitative analysis in 10 continuous layers, and then Mimics 15.0 software (Materialise, Belgium) was used for 3D reconstruction.

Histomorphometry analysis

After high-resolution microcomputer tomography, all specimens were placed in a centrifuge tube containing 10% EDTA decalcification solution (PH = 7.4) for 4 weeks, excess soft tissue on the specimens was removed, and the specimens were dehydrated in concentration gradient alcohol. Subsequently, all specimens were placed in n-butanol for 8 h and soaked in paraffin for 6 h. Finally, the paraffin block was cut into 6-micron-thick coronal sections with using a rotary paraffin slicer. The obtained sections were stained by H&E, SOFG, TB, and IHC. Quantitative analysis of articular cartilage damage of ankle joint and subtalar joint in mice was then carried out using the modified MANKIN score and the OA cartilage histopathological evaluation system of the Osteoarthritis Research Society International (OARSI) [28, 29]. Histological scores were performed by two independent senior readers on the tibialis and talus articular cartilage of the ankle, and on the talus and calcaneal articular cartilage of the subtalar joint. Five slides were used for each sample. The reliabilities of parameters obtained by the two researchers were calculated using the intraclass correlation coefficients (ICC). The modified MANKIN score and OARSI score showed good–excellent reliability (Modified Mankin scores for the ankle joints ICC(2,1) = 0.955; Modified Mankin scores for the subtalar joints ICC(2,1) = 0.977; OARSI scores for the ankle joints ICC(2,1) = 0.839; OARSI scores for the subtalar joints ICC(2,1) = 0.973). Finally, the histological scores were analyzed statistically.

Immunohistochemistry

Endogenous peroxidase was first blocked by incubation with 3% H_2O_2. Subsequently, enzymatic digestion was performed with 0.25% trypsin at 37 °C for 1 h for antigenic epitope repair. The reaction was then blocked by 10% goat serum for 1 h at room temperature. The sections were then incubated with primary antibody (anti-Collagen II; Abcam, Cambridge, MA)

overnight at 4 °C. Finally, the sections were incubated with HRP-conjugated secondary antibody, followed by color development with the DAB horseradish peroxidase chromogenic kit. The sections were washed and stained with hematoxylin. Finally, the area positive for type II collagen was analyzed with using ImageJ software.

Statistical analysis

SPSS v23.0 (SPSS Inc., Chicago, IL, USA) and GraphPad Prism 8.0 (GraphPad Software, La Jolla, CA, USA) were used for statistical analysis. With reference to Turner's previous study [30] and considering the sample size of our study, a two- way ANOVA (group x time) was used to determine the significance of the differences between the three groups included in the balance beam study. In this experiment, three comparisons were performed: 1. the SHAM group compared to the CFL laxity group; 2. the CFL laxity group compared to the DL laxity group; 3. the DL laxity group compared to the SHAM group. The Student's t-test was used to interpret statistical differences, and Bonferroni post hoc comparisons were performed between the each two groups. An alpha level of $P < 0.05$ was used to determine significant effects for each analysis. For other experimental data, the normality of distribution and homogeneity of variance of each group of data were tested first. One-way ANOVA analysis was conducted on each set of data, as it conformed to normal distribution and homogeneity of variance, and Tukey's HSD for post hoc testing was used. Data are expressed as means ± standard deviation (SD). Furthermore, $p < 0.05$ was considered to be statistically significant [10].

Results

Balance assessments

Each mouse was tested three times in the balance assessment at each stage, and the data of the three tests were recorded; the average values were used for subsequent statistical analysis.

The time required for mice to cross the balance beam was statistically analyzed at the same stage between groups. No statistically significant difference was observed in the time taken by the mice to pass the balance beam between the three groups before operation ($p = 0.599$, 0.660, 0.902, and > 0.05). The time required for CFL laxity group and DL laxity group mice to pass through the balance beam at three days, one week, 4 weeks, 8 weeks, and 12 weeks after surgery was significantly increased compared with that for the SHAM group ($p < 0.05$), whereas the time required for the CFL laxity group and DL laxity group mice to pass through the balance beam did not significantly differ ($p > 0.05$) (Fig. 2A).

Statistical analysis of the number of right hind foot slips of mice between groups at the same stage showed that there was no statistically significant difference in the number of slips from the balance beam between the three groups before operation ($p = 0.988$, 0.856, 0.830, > 0.05). On the third day after operation, the number of right hind foot slips from the balance beam in CFL laxity group and DL laxity group were higher than those in the SHAM group, and the difference was statistically significant ($p = 0.013$, 0.024, < 0.05). In contrast, the difference in number of right hind foot slips from the balance beam between the CFL laxity group and DL laxity group was not statistically significant ($p = 0.112$). The difference in the number of right hind foot slips of mice from the

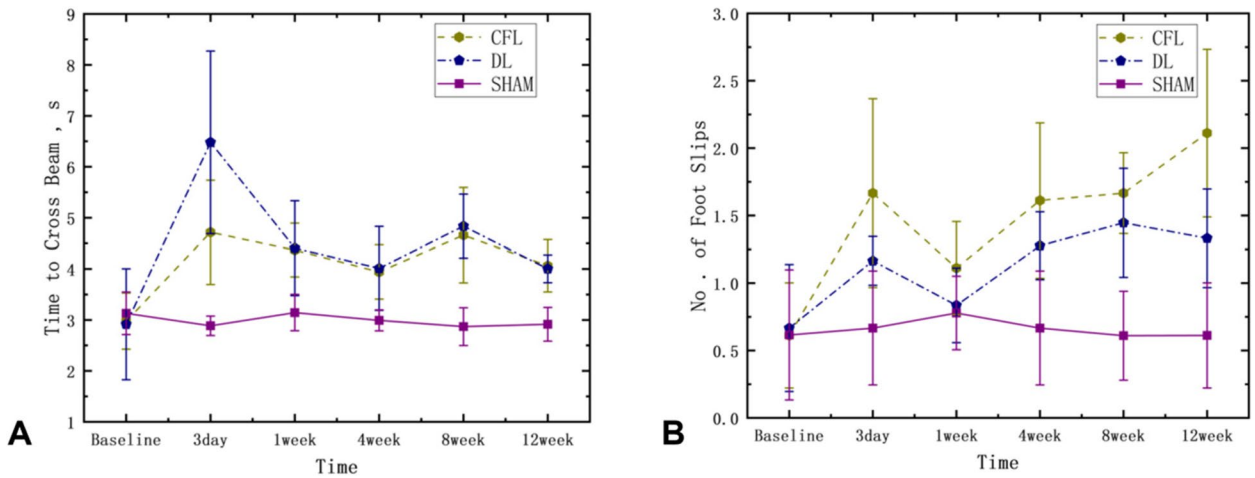

Fig. 2 Balance assessments of mice (means ± standard deviations). **A** Time required for mice to cross the balance beam. **B** Number of slips of the right hindfoot when traversing the balance beam

balance beam between groups was not significant one week after the operation ($p = 0.093$, 0.728, 0.155, > 0.05). At 4 weeks, 8 weeks, and 12 weeks after the operation, the number of slips in the CFL laxity group and DL laxity group was significantly higher than that in the SHAM group, and the difference was statistically significant ($p < 0.05$); However, there was no significant difference in the number of slips between the CFL laxity group and the DL laxity group, except at 12 weeks after operation ($p = 0.024$). There was no significant difference in the data at 4 and 8 weeks after the operation ($p = 0.221$, 0.309, > 0.05) (Fig. 2B).

Footprint analysis

The stride length and width of each mouse before and 12 weeks after the operation were measured and recorded for further statistical analysis. In the analysis, we found that the stride length and width of mice increased with an increase in age, but the CFL laxity group and DL laxity group also showed a shortened stride length and width. There was no statistically significant difference in the stride length and width of the right hind foot among the three groups of mice before the operation ($p > 0.05$). At 12 weeks after the operation, the stride length and width of the right hind foot in the CFL laxity group and DL laxity group mice were significantly shorter than those of the right hind foot in the SHAM group, and the difference was statistically significant ($p < 0.05$). However, there was no statistically significant difference in the stride length and width of the right hind foot between the CFL laxity group and the DL laxity group at 12 weeks after the operation ($p > 0.05$) (Fig. 3).

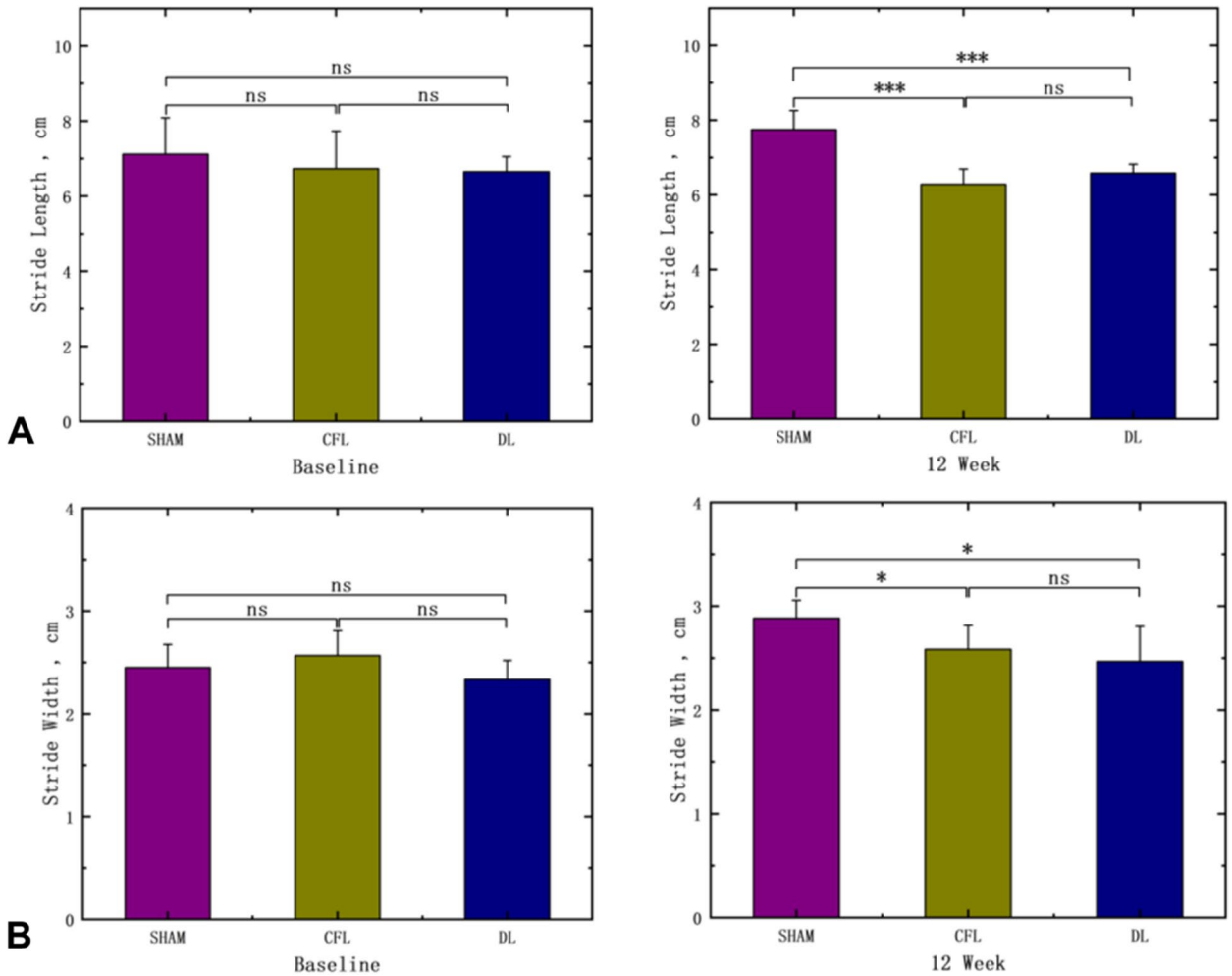

Fig. 3 Footprint analysis of mice (means ± standard deviations). **A** Stride length analysis of the right hind foot of mice in each group before and 12 weeks after surgery. **B** Stride width analysis of the right hind foot of mice in each group before and 12 weeks after surgery. (Note: *$P < 0.05$; **$P < 0.01$; ***$P < 0.001$; ****$P < 0.0001$; ns indicated that the difference was not statistically significant)

Micro-CT scanning

At 12 weeks after the operation, micro-CT scanning was performed on the cartilage layer of the ankle joint surface and the subtalar joint surface of the right hind limb of mice to quantitatively evaluate the subchondral bone. Three-dimensional reconstruction of CT images suggested that the ankle articular surface and subtalar articular surface of the CFL laxity group and DL laxity group were rough, worn, and defective, accompanied by the formation of osteophytes. This suggested that degenerative changes had occurred in the ankle and subtalar articular surface (Fig. 4A). In addition, the bone volume fraction (BV/TV) of the CFL laxity group and DL laxity group were significantly increased compared with that of the SHAM group ($p < 0.05$) (Fig. 4B). This indicated that the subchondral bone mass and bone density of the ankle and subtalar joints both increased, presenting an overall state of "ossification."

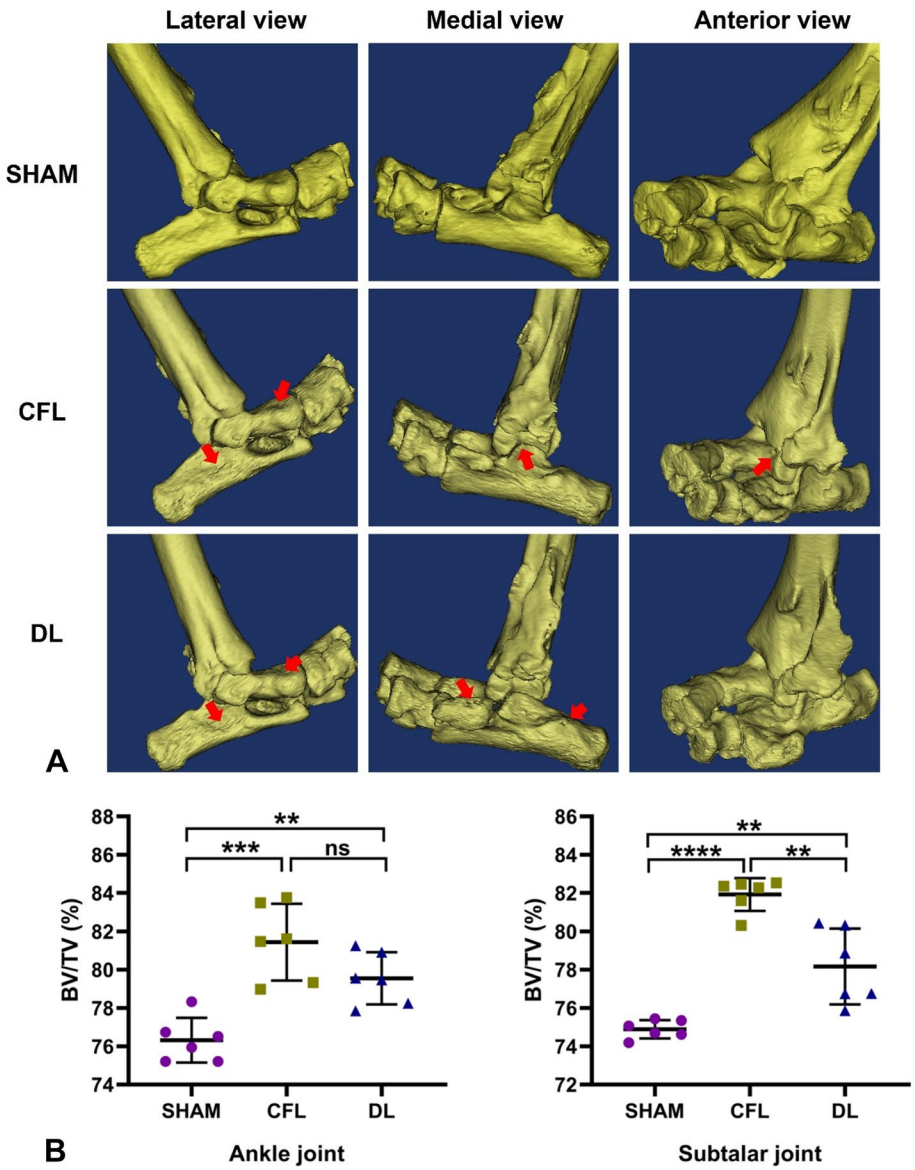

Fig. 4 Micro-CT analysis of mouse right feet. **A** Three-dimensional reconstruction of the ankle and the subtalar joint in mice (lateral view, medial view, and anterior view) (the surfaces of the joints in the CFL relaxation and the DL relaxation groups were rough: the black arrow points; Wear defects on the surface of the joint: the part indicated by the green arrow; Osteophyte formation on the surface of the joint: the area indicated by the red arrow). **B** Quantitative analysis of bone volume fraction (BV/TV) of the ankle joint and subtalar in mice. (Note: *$P < 0.05$; **$P < 0.01$; ***$P < 0.001$; ****$P < 0.0001$; ns indicated that the difference was not statistically significant)

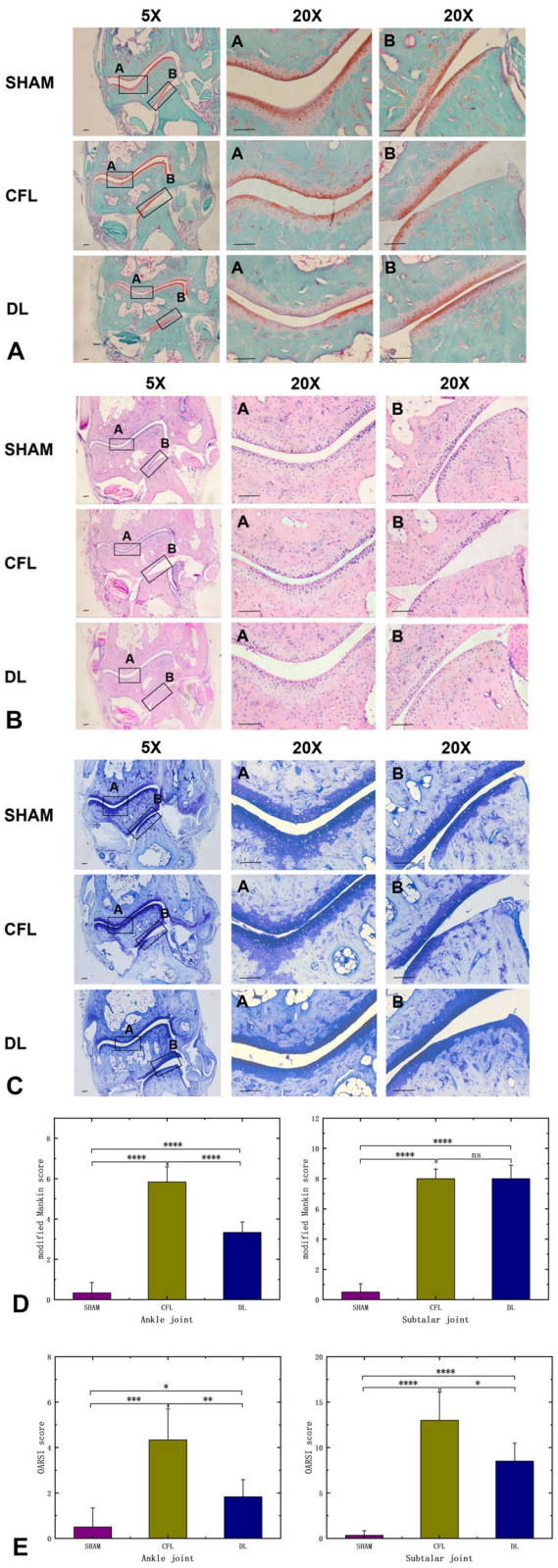

◀ **Fig. 5** Safranin O-Fast green and Hematoxylin and eosin (H&E) and toluidine blue staining and analysis of the ankle and subtalar joints. **A** Safranin O-Fast green staining of the ankle and subtalar joints in mice. **B** H&E staining of the ankle and subtalar joint in mice. **C** Toluidine blue staining of the ankle and subtalar joints in mice. **D** Modified Mankin scores for the ankle and subtalar joints in mice. **E** OARSI scores for the ankle and subtalar joints in mice. A ankle joint, B subtalar joint. Scale bar = 100 μm (Note: $^{*}P < 0.05$; $^{**}P < 0.01$; $^{***}P < 0.001$; $^{****}P < 0.0001$; ns indicated that the difference was not statistically significant)

Histomorphometry analysis

To further demonstrate that ankle instability can lead to osteoarthritis and damage the cartilage layer of the ankle and subtalar joints, we performed H&E staining, SOFG staining, TB staining, and IHC staining.

On observing the typical SOFG staining images of each group, the cartilage layer of the ankle joint and subtalar joint in the SHAM group was intact, with intact morphology, normal cell matrix structure, and intact cell morphology. In the CFL laxity group, the subtalar articular cartilage layer was defective, with more than one-third defect area, resulting in the local loss of safranin-O staining. The surface of the ankle joint cartilage layer was discontinuous, and the local cartilage layer became thinner. In the DL laxity group, the ankle cartilage layer surface was discontinuous, chondrocytes and cell matrix were significantly reduced, the coloration of safranin-O was weakened, and the degenerative pairs of subtalar joints were less severe (Fig. 5A). Further, on observing the typical H&E staining images of each group, the cartilage surface of the ankle joint and subtalar joint in the SHAM group was intact, with normal morphology, uniform distribution of chondrocytes, and normal staining of the cell matrix. However, in the CFL laxity group, the subtalar articular surface cartilage layer was obviously missing, the intrastromal coloration was reduced, the distribution of chondrocytes in the articular surface cartilage layer of the ankle was uneven, and the degeneration of cartilage was relatively mild. The number of chondrocytes in the ankle joint and the subtalar joint cartilage layer in the DL laxity group was reduced and unevenly distributed, and cell matrix staining was reduced, but the degeneration of cartilage was relatively milder than that observed in the CFL laxity group (Fig. 5B). On observing the typical TB staining images in each group, the cartilage layer of the ankle joint and subtalar joint in the SHAM group was intact, with normal morphology and complete cell morphology. However, in the CFL laxity group, the cartilage tissue of the subtalar articular surface was incomplete, with approximately one-third cartilage loss; the cartilage layer of the ankle was thinner, and the colored area was reduced. The DL laxity group had defects of the subtalar

articular surface cartilage layer, incomplete cartilage surface, and significantly reduced colored area. In contrast, the ankle articular cartilage layer became thinner, and the colored area decreased (Fig. 5C). The modified MANKIN score and OARSI score in the CFL laxity group and DL laxity group were significantly higher than those in the SHAM group and the difference was statistically significant ($p < 0.05$) (Fig. 5D, E).

In the IHC staining of typical type II collagen in each group, it could be seen that the content of type II collagen was uniform in the cartilage layer of the ankle joint and subtalar joint in the SHAM group. However, in the CFL laxity group, the content of type II collagen in the subtalar articular cartilage layer was significantly reduced and defective and that in the ankle articular cartilage layer was also reduced. In the DL laxity group, the area containing type II collagen in the cartilage layer of the ankle joint and subtalar joint was also significantly reduced (Fig. 6A). The ImageJ software was used to calculate the ratio of type II collagen-positive area to total visual field area in each visual field. It was found that the expression of type II collagen in the ankle and subtalar articular cartilage in the CFL laxity group and DL laxity group was significantly lower than that in the SHAM group, and the difference was statistically significant ($p < 0.001$) (Fig. 6B).

Discussion

Ankle sprain (AS) is one of the most common injuries in the process of sports. A sprain can lead to the relaxation or fracture of ligaments around the ankle joint, which causes a change in the mechanical properties of the ankle joint or the adjacent joints and further causes instability of the ankle joint or adjacent joints [31–33]. The current mouse models of ankle instability are established by cutting the ligaments that maintain the stability of the ankle joint [10, 20, 34, 35]. However, in actual clinical practice, most ankle instability patients do not have broken ligaments around the ankle joint, but rather the ligaments are in a relaxed state [36]. Therefore, we established a mouse model of ankle instability with ankle osteoarthritis with the help of relaxation of CFL and DL caused by the rapid descent of weights. Balance assessments and footprint analysis were performed to evaluate whether the motor level and balance ability of mice were impaired. In contrast, micro-CT scanning and histomorphometry analysis were performed to evaluate whether long-term ankle instability causes PTOA.

In this study, it was found that ligament laxity would lead to the degeneration of articular cartilage and then develop into osteoarthritis, which was similar to the results of osteoarthritis caused by transverse ligament dissection. Compared with previous studies, it was found that within 8 weeks, the time of passing the balance beam was similar between the ligamentous relaxation group and the ligamentous transverse section group [10]. At the 12th week, the time for the ligament laxity group to pass the balance beam was shorter than that for the ligament transverse section group. However, different molding methods did not affect the number of slides [10, 34]. By comparing the OARSI score and the modified Mankin score of the ankle and subtalar joints after ligament transection and ligament relaxation, the score was higher after ligament transection, indicating that the degenerative changes of articular cartilage were more significant after ligament transection [10]. However, different molding methods had no significant effect on the expression of type II collagen. In addition, different molding methods have different effects on the bone volume fraction of ankle joint and subtalar joint. The results showed that the bone volume fraction of the transverse ligament group was similar to that of the CFL laxity relaxation group, but the bone volume fraction increased significantly compared with that of the DL ligament relaxation group [37]. In general, ligament relaxation can lead to ankle instability, and then develop osteoarthritis, but its severity is not as severe as the transverse ligament model.

Balance assessments

With regard to the time required to pass the balance beam, the CFL laxity group and DL laxity group required significantly longer time than the SHAM group at three days and one week after surgery. This phenomenon may be because of the obvious edema and pain in the right hind foot ankle joint of mice in the early stage after surgery. This resulted in the slowing down of the mouse crawling on the balance beam owing to pain feedback and relatively increased the time taken. This suggests that physical activity levels should be reduced early after an acute ankle injury, as the Hubbard-Turner study reported that rest after a severe ankle sprain is essential to restore physical activity levels throughout the life cycle [38]. At postoperative 4 weeks, the time difference between the CFL and DL laxity groups and the SHAM group for crossing the balance beam was minimal. At this time, the surgical incision at the right hind foot ankle joint was completely healed, and the soft tissue swelling had completely subsided. At the later stage of the study (8 weeks after surgery), mice in the CFL and DL laxity groups took longer to traverse the balance beam than those in the SHAM group, which is consistent with what was observed after the transection of the ligaments around the ankle [10, 30, 34, 39]. At this time, the right hind foot ankle joint of mice was significantly deformed, and the stiffness of the joint caused instability in the right hind foot, possibly reducing the speed of the mice while crossing the balance beam.

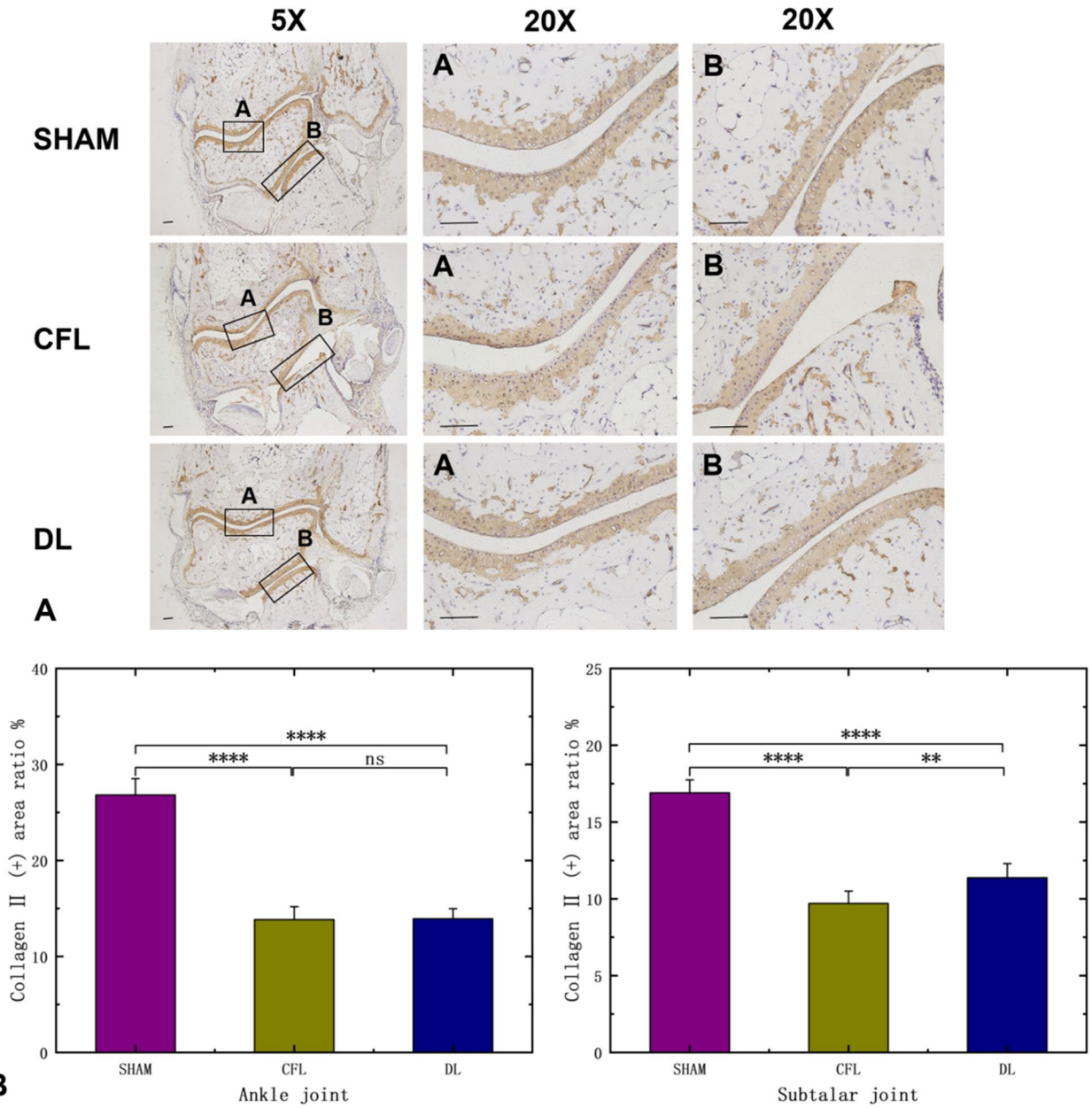

Fig. 6 Type II collagen immunohistochemical staining and analysis of the ankle and subtalar joints. **A** Type II collagen immunohistochemical staining of the subtalar joints in mice. **B** Collagen II (+) area ratio percentage for the subtalar joints in mice. A ankle joint, B subtalar joint. Scale bar = 100 μm (Note: *$P < 0.05$; **$P < 0.01$; ***$P < 0.001$; ****$P < 0.0001$; ns indicated that the difference was not statistically significant)

With regard to the number of slips from the balance beam, the number of slips of the right hind foot in the CFL laxity group and DL laxity group were significantly higher than those in the SHAM group at 3 days, 4 weeks, 8 weeks, and 12 weeks after surgery.However, there was no significant difference between the two groups at 1 week after surgery. The reason for this phenomenon may be that the ankle joint edema of mice decreased 1 week after surgery, and the number of slips decreased owing to the slow speed because of pain when crawling across the balance beam. At 12 weeks after surgery, the number of slips of the right hind foot in the CFL laxity group mice was 3.45 times that observed before surgery, and the number of slips of the right hind foot in the DL laxity group mice was 1.99 times that observed before surgery. The number of slips of the right hind foot in the CFL laxity group mice was 1.58 times that observed in the DL laxity group mice. These results are similar

to the experimental results observed by the Hubbard Turner research group by cutting the ligaments around the ankle joint [30, 39]. At this point, the mouse may have progressed from long-term chronic ankle instability to PTOA. Previous studies have shown that individuals with PTOA have balance disorders and changes in movement patterns, which are consistent with our experimental results [40, 41]. In the whole postoperative balance beam experiment, the right hind foot of mice in the CFL laxity group slipped slightly more than that of mice in the DL laxity group, and the difference was statistically significant 12 weeks after surgery. This also reflected that CFL, as the only ligament connecting the tibiotalar joint and subtalar joint at the same time, plays an important role in maintaining the stability of both ankle and subtalar joints [10, 42, 43].

Footprint analysis

The stride length and stride width data measured at 12 weeks in the SHAM group were greater than those observed before surgery. During the study period, the mice continued to grow, leading to individual enlargement and corresponding increases in stride length and width. However, although the mice in the CFL laxity group and DL laxity group grew larger, the stride length and stride width did not show an increase but rather decreased compared with those before surgery. They were significantly shortened compared with the stride length and width in the SHAM group in the same period. The research results suggest that CFL and DL relaxation can cause ankle instability, thereby affecting the normal gait of mice, similar to the results reported by the Hubbard Turner research team wherein the gait of mice was damaged by cutting the lateral ligament of the ankle [39].

Micro-CT scanning

Under normal physiological conditions, osteoclast bone resorption and osteoblast bone formation maintain the dynamic balance of the bone state. Micro-CT quantitative analysis showed that the ankle bone volume fraction in the CFL laxity group and DL laxity group was 6.71% and 4.23% higher than that in the SHAM group, respectively. These results indicated that the relaxation of the ligament around the right hind foot ankle joint in mice broke the stable bone balance, resulting in the abnormal activity of osteoblasts, increased bone density, bone hyperplasia, subchondral bone hardening and thickening, and degenerative changes at the joint site. This result is similar to the CT analysis results of Chang et al. [20], who established the ankle osteoarthritis model through surgery. In addition, in the process of CT image reconstruction and analysis, degenerative changes also occurred in the subtalar joint of mice. The bone volume fractions of the subtalar joint in the CFL laxity group and DL laxity group were 9.39% and 4.37% higher than those of the subtalar joint in the SHAM group, respectively. This result is consistent with the results of previous studies showing that severe foot instability can lead to the degeneration of adjacent ankle joints, suggesting that ankle joint instability in the animal model in this study is more serious [10, 44].

Histomorphometry analysis

In typical H&E staining, SOFG staining, and TB staining, obvious discontinuity was observed on the ankle surface in the CFL laxity group and DL laxity group. The number of chondrocytes on the joint surface was lower or chondrocytes had completely disappeared, and there were empty nucleated chondrocytes, suggesting that ligament relaxation could lead to ankle instability. Ankle instability without effective treatment can lead to PTOA. The results are similar to those obtained by cutting the ligaments around the ankle in mice to construct animal models of ankle instability and ankle osteoarthritis [10, 20]. In addition, large defects were also observed on the surface of subtalar joints in the CFL laxity group. In contrast, damage to subtalar joints in the DL laxity group was less than that in the CFL laxity group. This phenomenon may be caused by the fact that CFL connects the tibial talar joint and the subtalar joint at the same time [10, 42, 43], and its relaxation not only causes ankle injury but also damages the subtalar joint to some extent. In fact, the ankle joint and the subtalar joint are two inseparable structures, which can be called the ankle-subtalar joint complex. Hence, the subtalar joint surface in the DL laxity group also had certain injuries, which was similar to the results reported by Liu et al. [10] In typical type II collagen immunohistochemical staining, the type II collagen-positive area in the ankle joint and subtalar articular cartilage layer in the CFL laxity group and DL laxity group was significantly reduced compared with that in the SHAM group. This difference may be caused by the destruction of some articular chondrocytes, which fail to normally produce type II collagen. Type II collagen is a type of high molecular weight protein produced by articular chondrocytes, which can produce certain mechanical strength to maintain the normal physiological function of articular cartilage. When articular chondrocytes are destroyed, the production of type II collagen also decreases. This result was consistent with the results of the abovementioned three staining methods and with the results of Liang et al. [45], who constructed a rat model of post-traumatic osteoarthritis through ankle fracture.

In this study, the effects of chronic ankle instability after grade I ankle sprain on post-traumatic osteoarthritis

were described from macroscopic and microscopic levels. From a macro perspective, we found through behavioral experiments, including balance beam experiment and gait analysis, that the balance ability of mice decreased after ligament relaxation led to chronic ankle instability. On the micro level, we found that ankle sprain would lead to chronic ankle instability and further develop into degenerative changes of the joint, specifically manifested as the reduction of chondrocytes and the reduction of type II collagen positive area. In addition, Micro-CT results also indicated increased bone density and subtalar bone ossification in the ankle and subchondral joints. The macro instability of the mouse ankle joint leads to the abnormal stress stimulation of the mouse ankle, which results in the degeneration of the joint and the ossification of the cartilage at the micro level.

Limitations

There are some limitations to the study. First, the animal used in the experiment is mice. Although the structure of the hind foot and ankle joint of mice is similar to that of humans, it should be noted that mice are quadruped, while humans are biped. Thus, the consistency of movement patterns and behavior needs to be further verified and studied. Second, this study needs to further elucidate the signaling pathway and molecular mechanisms of joint degeneration at a cellular level. More in-depth studies and more reasonable animal models should be developed in future studies.

Conclusions

The results of this study showed that chronic ankle instability induced by grade I ankle sprain impairs motor coordination and balance in mice, and eventually can induce PTOA of the ankle and its adjacent joints. This model could provide a new understanding of how grade I ankle sprains develops into chronic articular cartilage degeneration and paves the way for the related research on subtalar osteoarthritis in the future.

Abbreviations

CAI	Chronic ankle instability
PTOA	Post-traumatic osteoarthritis
CFL	Calcaneofibular ligament
DL	Deltoid ligament
AS	Ankle sprain
ATFL	Anterior talofibular ligament
PTFL	Posterior talofibular ligament
H&E	Hematoxylin and Eosin
SOFG	Safranin O-Fast Green
TB	Toluidine blue
SPF	Specific Pathogen Free
IHC	Immunohistochemistry

Acknowledgements

NA.

Authors' contributions

J.Y.and Y.D. designed the Conceptualization, developed the methodology and collected the data. Y.D.and F. Y. and S. W. prepared the Behavioral Assessment. F.Y.and H. X. and Y. C. performed the data Statistical analysis and writing original draft preparation. All authors have read and agreed to the published version of the manuscript.

Funding

This work was supported by the Jiangsu provincial government scholarship program and the Priority Academic Program Development of Jiangsu Higher Education Institutions (PAPD).

Availability of data and materials

Images and datasets used and/or analyzed during the current study are available from the corresponding author on reasonable request.

Data availability

No datasets were generated or analysed during the current study.

Declarations

Ethics approval and consent to participate

All procedures followed the NIH Guide for the Care and Use of Laboratory Animals and were approved by the Medical Ethics Committee of the First Affiliated Hospital of Soochow University (protocol code 296–2023).

Consent for publication

This manuscript has not been published and is not under consideration for publication elsewhere.

Competing interests

The authors declare no competing interests.

Author details

[1]Department of Orthopedic Surgery, School of Biology and Basic Medical Sciences, Orthopedic Institute, The First Affiliated Hospital, Suzhou Medical College, Soochow University, 899 Pinghai Road, Suzhou, Jiangsu 215007, People's Republic of China. [2]School of Physical Education and Sports, Soochow University, 50 Donghuan Road, Suzhou, Jiangsu 215006, People's Republic of China. [3]Emergency and Critical Care Center, Intensive Care Unit, Zhejiang Provincial People's Hospital (Affiliated People's Hospital), Hangzhou Medical College, 158 Shangtang Road, Hangzhou, Zhejiang 314408, People's Republic of China.

Received: 24 June 2024 Accepted: 15 September 2024
Published online: 28 September 2024

References

1. Waterman BR, Belmont PJ Jr, Cameron KL, Deberardino TM, Owens BD. Epidemiology of ankle sprain at the United States Military Academy. Am J Sports Med. 2010;38(4):797–803.
2. Fong DT, Chan YY, Mok KM, Yung PS, Chan KM. Understanding acute ankle ligamentous sprain injury in sports. Sports Med Arthrosc Rehabil Ther Technol. 2009;1:14.
3. Herzog MM, Kerr ZY, Marshall SW, Wikstrom EA. Epidemiology of ankle sprains and chronic ankle instability. J Athl Train. 2019;54(6):603–10.
4. Medina McKeon JM, Hoch MC. The ankle-joint complex: a kinesiologic approach to lateral ankle sprains. J Athl Train. 2019;54(6):589–602.
5. Jones MH, Amendola AS. Acute treatment of inversion ankle sprains: immobilization versus functional treatment. Clin Orthop Relat Res. 2007;455:169–72.
6. Anandacoomarasamy A, Barnsley L. Long term outcomes of inversion ankle injuries. Br J Sports Med. 2005;39(3):e14 discussion e14.
7. Karlsson J, Eriksson BI, Renström P. Subtalar instability of the foot. A review and results after surgical treatment. Scand J Med Sci Sports. 1998;8(4):191–7.
8. Kleipool RP, Stufkens SAS, Dahmen J, Vuurberg G, Streekstra GJ, Dobbe JGG, Blankevoort L, Knupp M. Difference in orientation of the talar

articular facets between healthy ankle joints and ankle joints with chronic instability. J Orthop Res. 2022;40(3):695–702.
9. Keefe DT, Haddad SL. Subtalar instability. Etiology, diagnosis, and management. Foot Ankle Clin. 2002;7(3):577–609.
10. Liu P, Chen K, Wang S, Hua C, Zhang H, Yu J. A mouse model of ankle-subtalar joint complex instability induced post-traumatic osteoarthritis. J Orthop Surg Res. 2021;16(1):541.
11. Yang N, Waddington G, Adams R, Han J. Age-related changes in proprioception of the ankle complex across the lifespan. J Sport Health Sci. 2019;8(6):548–54.
12. Close JR. Some applications of the functional anatomy of the ankle joint. J Bone Joint Surg Am. 1956;38-a(4):761–81.
13. Swenson DM, Collins CL, Fields SK, Comstock RD. Epidemiology of U.S. high school sports-related ligamentous ankle injuries. Clin J Sport Med. 2013;23(3):190–6 2005/06–2010/11.
14. Campbell KJ, Michalski MP, Wilson KJ, Goldsmith MT, Wijdicks CA, LaPrade RF, Clanton TO. The ligament anatomy of the deltoid complex of the ankle: a qualitative and quantitative anatomical study. J Bone Joint Surg Am. 2014;96(8): e62.
15. Stufkens SA, van den Bekerom MP, Knupp M, Hintermann B, van Dijk CN. The diagnosis and treatment of deltoid ligament lesions in supination-external rotation ankle fractures: a review. Strat Trauma Limb Reconstr. 2012;7(2):73–85.
16. Earll M, Wayne J, Brodrick C, Vokshoor A, Adelaar R. Contribution of the deltoid ligament to ankle joint contact characteristics: a cadaver study. Foot Ankle Int. 1996;17(6):317–24.
17. Harper MC. An anatomic study of the short oblique fracture of the distal fibula and ankle stability. Foot Ankle. 1983;4(1):23–9.
18. Michelson JD, Varner KE, Checcone M. Diagnosing deltoid injury in ankle fractures: the gravity stress view. Clin Orthop Relat Res. 2001;387:178–82.
19. Fang H, Beier F. Mouse models of osteoarthritis: modelling risk factors and assessing outcomes. Nat Rev Rheumatol. 2014;10(7):413–21.
20. Chang SH, Yasui T, Taketomi S, Matsumoto T, Kim-Kaneyama JR, Omiya T, Hosaka Y, Inui H, Omata Y, Yamagami R, et al. Comparison of mouse and human ankles and establishment of mouse ankle osteoarthritis models by surgically-induced instability. Osteoarthritis Cartilage. 2016;24(4):688–97.
21. Charles JP, Cappellari O, Spence AJ, Wells DJ, Hutchinson JR. Muscle moment arms and sensitivity analysis of a mouse hindlimb musculoskeletal model. J Anat. 2016;229(4):514–35.
22. Gao C, Chen Z, Cheng Y, Li JK, Huang XW, Wei LY, He F, Luo ZP, Zhang HT, Yu J. Comparative anatomy of the mouse and human ankle joint using Micro-CT: Utility of a mouse model to study human ankle sprains. Math Biosci Eng. 2019;16(4):2959–72.
23. Kaikkonen A, Kannus P, Järvinen M. A performance test protocol and scoring scale for the evaluation of ankle injuries. Am J Sports Med. 1994;22(4):462–9.
24. Criscenti G, De Maria C, Sebastiani E, Tei M, Placella G, Speziali A, Vozzi G, Cerulli G. Quasi-linear viscoelastic properties of the human medial patello-femoral ligament. J Biomech. 2015;48(16):4297–302.
25. Ashton-Miller JA, Ottaviani RA, Hutchinson C, Wojtys EM. What best protects the inverted weightbearing ankle against further inversion? Evertor muscle strength compares favorably with shoe height, athletic tape, and three orthoses. Am J Sports Med. 1996;24(6):800–9.
26. Wikstrom EA, Hubbard-Turner T, Duncan A, Cline J, Turner MJ. Prolonged rest, long-term dynamic balance, and gait in a mouse ankle-sprain model. J Athl Train. 2019;54(7):801–7.
27. Wikstrom EA, Hubbard-Turner T, Guderian S, Turner MJ. Lateral ankle sprain in a mouse model: lifelong sensorimotor dysfunction. J Athl Train. 2018;53(3):249–54.
28. Naito K, Watari T, Furuhata A, Yomogida S, Sakamoto K, Kurosawa H, Kaneko K, Nagaoka I. Evaluation of the effect of glucosamine on an experimental rat osteoarthritis model. Life Sci. 2010;86(13–14):538–43.
29. Gerwin N, Bendele AM, Glasson S, Carlson CS. The OARSI histopathology initiative - recommendations for histological assessments of osteoarthritis in the rat. Osteoarthritis Cartilage. 2010;18(Suppl 3):S24-34.
30. Hubbard-Turner T, Wikstrom EA, Guderian S, Turner MJ. Acute ankle sprain in a mouse model. Med Sci Sports Exerc. 2013;45(8):1623–8.
31. Ardakani MK, Wikstrom EA, Minoonejad H, Rajabi R, Sharifnezhad A. Hop-stabilization training and landing biomechanics in athletes with chronic ankle instability: a randomized controlled trial. J Athl Train. 2019;54(12):1296–303.
32. Czajka CM, Tran E, Cai AN, DiPreta JA. Ankle sprains and instability. Med Clin North Am. 2014;98(2):313–29.
33. Chang SH, Morris BL, Saengsin J, Tourné Y, Guillo S, Guss D, DiGiovanni CW. Diagnosis and treatment of chronic lateral ankle instability: review of our biomechanical evidence. J Am Acad Orthop Surg. 2021;29(1):3–16.
34. Wang S, Liu P, Chen K, Zhang H, Yu J. Mouse model of subtalar post-traumatic osteoarthritis caused by subtalar joint instability. J Orthop Surg Res. 2022;17(1):537.
35. Li J, Chen Z, Cheng Y, Gao C, Li J, Gu X, He F, Luo Z, Yang H, Zhang H, et al. Ligamentous injury-induced ankle instability causing posttraumatic osteoarthritis in a mouse model. BMC Musculoskelet Disord. 2022;23(1):223.
36. Liu W, Li H, Hua Y. Quantitative magnetic resonance imaging (MRI) analysis of anterior talofibular ligament in lateral chronic ankle instability ankles pre- and postoperatively. BMC Musculoskelet Disord. 2017;18(1):397.
37. Wang S, Liu P, Hua C, Zhang H, Yu J. A Mouse Model of Ankle-Subtalar Complex Joint Instability. J Vis Exp. 2022(188):e64481.
38. Hubbard-Turner T, Wikstrom EA, Turner MJ. A 14-day recovery and physical activity levels after an ankle sprain in mice. J Athl Train. 2019;54(7):796–800.
39. Hubbard-Turner T, Wikstrom EA, Guderian S, Turner MJ. An acute lateral ankle sprain significantly decreases physical activity across the lifespan. J Sports Sci Med. 2015;14(3):556–61.
40. OMcKeon P. dynamic systems theory as a guide to balance training development for chronic ankle instability: a review of the literature. Athletic Train Sports Health Care. 2012;4(5):230–6.
41. Koo ST, Park YI, Lim KS, Chung K, Chung JM. Acupuncture analgesia in a new rat model of ankle sprain pain. Pain. 2002;99(3):423–31.
42. Kjaersgaard-Andersen P, Wethelund JO, Nielsen S. Lateral talocalcaneal instability following section of the calcaneofibular ligament: a kinesiologic study. Foot Ankle. 1987;7(6):355–61.
43. Li L, Gollhofer A, Lohrer H, Dorn-Lange N, Bonsignore G, Gehring D. Function of ankle ligaments for subtalar and talocrural joint stability during an inversion movement - an in vitro study. J Foot Ankle Res. 2019;12:16.
44. Zhi C, Ting L, Junkun L, Chao G, Fan H, Zongping L, Huilin Y, Hongtao Z, Jia Y. Early detection of joint degeneration in the subtalar and talonavicular joints secondary to ankle instability in a mouse model. Med Novel Technol Devices. 2021;11:100080.
45. Liang D, Sun J, Wei F, Zhang J, Li P, Xu Y, Shang X, Deng J, Zhao T, Wei L. Establishment of rat ankle post-traumatic osteoarthritis model induced by malleolus fracture. BMC Musculoskelet Disord. 2017;18(1):464.

Publisher's Note